



OPEN

Genomic characterization of *Leishmania (V.) braziliensis* associated with antimony therapeutic failure and variable in vitro tolerance to amphotericin B

Laura Natalia Gonzalez-Garcia¹, Aura María Rodríguez-Guzmán²,
 Carolina M. Vargas-León³, Samanda Aponte³, Liliana A. Bonilla-Valbuena³,
 J. Manuel Matiz-González³, Ana M Clavijo-Vanegas³, Germán Andrés Duarte-Olaya²,
 Catherine Aguilar-Buitrago³, Daniel Alfonso Urrea², Jorge Duitama¹ & María C. Echeverry^{3,4}✉

Leishmaniasis, a vector-borne disease caused by protozoa from the *Leishmania* genus, presents a wide range of clinical manifestations in humans and varying responses to treatments. The main clinical presentations correspond with visceral leishmaniasis (VL), cutaneous leishmaniasis (CL), and mucosal leishmaniasis (ML). Amphotericin B (AmB) is a second-line therapeutic option in all forms of leishmaniasis with treatment failure or contraindication for Antimony derivates (SbV) therapy and in geographical regions with a high prevalence of SbV-resistant parasites. This study delves into the genomic features of thirteen *L. (V.) braziliensis* clinical isolates from CL patients who experienced therapeutic failure to SbV treatment. The isolates were categorized based on their AmB in vitro susceptibility in the amastigote stage, the intracellular parasitic form found in the vertebrate host. The whole genome sequences of the isolates were analyzed and compared with the reference genomes of *L. (V.) braziliensis* (MHOM/BR/75/M2904 and M2903). The average number of heterozygous SNPs in clinical isolates is at least 75% higher than the reference genomes, and the allele dosages suggest an overall ploidy of two, except in chromosome 31. The main mutations associated with AmB resistance previously reported in experimental cell lines from *L. (L.) infantum*, *L. (L.) mexicana*, and *L. (L.) donovani* were not found in this study. However, there were found mutations referred by other authors in parasites resistant to antileishmanial drugs in proteins such as GP63 (leishmanolysin), NADH-ubiquinone oxidoreductase- ESSS subunit- (putative), quinonoid dihydropteridine reductase, 20s proteasome beta 7 subunit- (putative), biotin transporter- (putative), and common hypothetical proteins. CNV analysis revealed that the isolates most tolerant to AmB present duplications of genomic regions encompassing genes involved in N-Glycan biosynthesis and biotin/folate transport and metabolism. Therefore, the present study uncovers previously undescribed metabolic pathways that could be involved in the natural AmB tolerance in *Leishmania*, which need to be functionally evaluated. These findings highlight the need for further drug response studies in field isolates.

Keywords *Leishmania braziliensis*, Cutaneous leishmaniasis, Resistance, Amphotericin B, Genome, Biotin, Dolichol phosphate mannose synthase

Protozoa parasites from the *Leishmania* genus infect human hosts through the bite of phlebotomine sandflies, producing a disease known as leishmaniasis that affects populations from tropical and subtropical regions in 98 countries¹. The parasite presents two physiologically different life stages: the promastigote in the invertebrate host and the amastigote, the intracellular form in the vertebrate host. In humans, leishmaniasis has three major

¹Systems and Computing Engineering Department, Universidad de los Andes, Bogotá, Colombia. ²Laboratorio de Investigaciones en Parasitología Tropical (LIPT), Universidad del Tolima, Ibagué, Colombia. ³Departamento de Salud Pública, Facultad de Medicina, Universidad Nacional de Colombia – Sede Bogotá, Bogotá, Colombia. ⁴Universidad Nacional de Colombia, Of. 303-Edif 471- Cr 30 45 – 03, Bogotá, Colombia. ✉email: mcheverryg@unal.edu.co

clinical manifestations: visceral leishmaniasis (VL), cutaneous leishmaniasis (CL), and mucosal leishmaniasis (ML). Based on *Leishmania*'s developmental pattern in the sandfly vector, the main species associated with human infections are divided into two subgenera: *Leishmania* Leishmania L. (L.) and *Leishmania* Vianna L. (V.)².

The treatment for leishmaniasis is limited to medicines with variable effectiveness and high toxicity. Salts of pentavalent antimony (SbV) persist as a first line of treatment for CL in many places. Their effectiveness varies depending on the parasite species, geographical origin, and the immunological condition of the patient³. In CL cases associated with the L. (V.) subgenus, the effectiveness of SbV derivatives is estimated at 75%⁴, while in CL and VL produced by species belonging to the L. (L.) subgenus, the rate of SbV-based treatment success ranges from 41 to 88%^{5,6}. When these drugs fail, or in epidemiologic scenarios of high resistance to SbV, lipidic Amphotericin B (L-AmB) formulations are the primary therapeutic approach to treat leishmaniasis¹. The cure rate in immunocompetent patients suffering from VL associated with L. (L.) subgenus treated with L-AmB ranges from 89 to 100%⁷. Analysis of the relationship between dose, intralesional AmB concentrations, and response after L-AmB treatment in murine models infected with L. (L.) major supports its use to treat CL⁸. However, L-AmB presents highly variable effectiveness in CL cases associated with L. (V.) subgenus in immunocompetent patients, ranging from 50 to 88.5%⁹⁻¹¹.

Therapeutic failure as a clinical response to leishmaniasis treatment, even in cases with a completed therapeutic scheme, does not necessarily mean parasite resistance. However, field isolates resistant to SbV have been found in Asia^{12,13}, North Africa¹⁴, and Latin America¹⁵. In addition, clinical isolates with low susceptibility to AmB have been reported in L. (L.) infantum from Uruguay¹⁶ and Brazil¹⁷, L. (L.) donovani in India¹⁸⁻²¹, and L. (V.) braziliensis and L. (V.) panamensis in Colombia²².

Field isolates and experimentally developed resistant strains to SbV show gene mutations related to membrane transport, efflux pumps, and antioxidant response²³. AmB resistance-associated genes have been found mainly as Lab-induced resistant promastigotes of species belonging to the L. (L.) subgenera. Those genes encode for proteins associated with the ergosterol synthesis pathway²⁴⁻²⁷, antioxidative response^{26,28-33}, and the membrane P-type ATPase transporter^{26,34}. However, the mechanisms associated with AmB tolerance in clinical isolates from L. (V.) subgenera are poorly understood. It is a problem of great relevance, given that AmB remains the last therapeutic alternative to treat complicated cases of CL and ML and for pediatric and immunosuppressed patients.

This study aimed to describe genomic changes potentially associated with AmB tolerance in clinical isolates of L. (V.) braziliensis. Thirteen clinical isolates previously evaluated for in vitro response to SbV³⁵ were classified as AmB-tolerant or AmB-susceptible in both promastigote and amastigote life stages. Whole genome sequencing analysis was performed, and missense SNPs and duplicated genomic regions containing a new set of genes potentially involved in AmB tolerance were identified.

Materials and methods

Parasites culture, U937 infections, and DNA preparation

The study involves 13 L. (V.) braziliensis clinical isolates belonging to the biobank of the *Laboratorio de parasitología-Facultad de Medicina -Universidad Nacional de Colombia*, derived from cutaneous lesions of Colombian patients diagnosed with CL, who presented therapeutic failure to Glucantime® treatment³⁵ and MHOM/BR/75/M2903 (M2903) acquired from ATCC. For the present study, the parasites were short-term (less than 10 in vitro passages after isolation) cultured in Schneider's Insect Medium (Sigma-Aldrich) supplemented with 10% fetal bovine serum (FBS, Gibco) and 1% Penicillin-Streptomycin (p/s, Lonza, cat 17-602) at 27 °C. Parasite growth was evaluated by daily cell counting in the Neubauer chamber. Two biological replicas and three technical replicates were counted for each isolate for seven days, and the data obtained was tabulated using Excel (Microsoft Corporation™).

Genomic DNA was prepared from 1×10^8 promastigotes using a QIAamp DNA mini kit (Qiagen, Cat #51306). DNA concentration was assessed by Qubit™ dsDNA HS and BR Assay Kits (Invitrogen, Cat # Q32851), and DNA quality was assessed by NanoDrop (Thermo Scientific™ NanoDrop™ One/OneC Microvolume UV-Vis Spectrophotometer, Cat # ND-ONE-W) and Ethidium Bromide-stained agarose gel. For Illumina sequencing, 250 ng of gDNA were sent to Macrogen Inc. Short-read whole-genome shotgun sequencing was performed, generating paired-end Illumina Hiseq (3₅₀ bp insert size, 100 bp read length) reads.

U937 monocytes were cultured in RPMI medium (Sigma-Aldrich) supplemented with 10% FBS (Gibco), 50 units/mL of penicillin, and 50 µg/mL of streptomycin at 37 °C and 5% CO₂. U937-derived macrophages were obtained by incubating 4×10^5 cells/mL for five days with 100 ng/mL (160nM) phorbol 12-myristate 13-acetate (PMA, Santa Cruz Biotechnology) on glass coverslips planted in 24-well plates. Adherent macrophages were incubated for 2 h with stationary promastigotes opsonized with AB + human serum in a 1:10 MOI in serum-free RPMI medium. The excess parasites were removed by three washes with incomplete RPMI, and infected cells were incubated for 24 h at 34 °C and 5% before further experiments.

Promastigote susceptibility assays

A resazurin viability assay addressed promastigote susceptibility to AmB (Sigma-Aldrich- Amphotericin B Cat A2942). 1×10^6 parasites/mL were seeded in 96-well plates with a 2-fold dilution series of AmB from 0.758 µM to 0.0015 µM and a control without AmB. After 42 h, resazurin (Sigma) in phosphate-buffered saline (PBS) was added to a final concentration of 12.5 µg/mL per well, and the plates were incubated for a further 6 h at 27°C. Resorufin fluorescence was measured in a Fluoroskan™ Microplate Fluorometer (Thermo Scientific™) at an excitation/emission wavelength of 543/590 nm. Data was processed in Microsoft Excel, and nonlinear regression analysis was conducted with GraphPad Prism to assess the promastigotes' AmB-EC₅₀.

Amastigote susceptibility assays

U-937 cells were infected, as previously mentioned. 24 hours post-infection (hpi), they were treated with increasing concentrations of AmB (Sigma-A9528). Concentration used (0; 0.011; 0.133; 0.332; 0.71, and 2.856 μ M), the drug was replenished at 48 hours post-treatment (hpt), and the susceptibility was assessed at 96hpt (120hpi). RNA was extracted using Direct-zol RNA Miniprep (Zymo Research). Relative quantification of *Leishmania* amastigotes was done using a modified protocol of the duplex RT-qPCR described by van den Bogaart et al. 2013³⁶. Briefly, one-step RT-qPCR was performed using Luna[®] Universal qPCR Master Mix (New England BioLabs) in an Applied Biosystems 7500 thermocycler. For *Leishmania* detection, 18S was amplified using the forward primer 5'-CCAAAGTGTGCAGATCGAAG-3', the reverse primer 5' GGCCGGTAAAGG CCGAATAG-3', and the probe 5'-FAM-ACCATTGTAGTCCACACTGC-BHQ1-3'. For macrophages, human β -2-microglobulin (β 2M) was amplified using the forward primer 5'-GCTCGCGCTACTCTCTCTT-3', the reverse primer 5'-CTCTGCTGGATGACGTGAGT-3', and the probe 5'-HEX-CGCTGGATAGCCTCCAGGC C-BHQ2-3'. $2^{-\Delta\Delta CT}$ was calculated for amastigotes' relative quantification using macrophages β 2M as a reference gene and *Leishmania* spp. 18 S as the target gene. Data were processed in Microsoft Excel, and nonlinear regression analysis was carried out with GraphPad Prism to assess the Amb-EC₅₀ in amastigotes.

Statistic methods

Parasite growth was analyzed by adjusting the Log2 transformed data to the exponential growth with the log (population) regression model to obtain the doubling time as an indicator value. To assess AmB susceptibility, represented as the Amb-EC₅₀ value, promastigotes viability, and $2^{-\Delta\Delta CT}$ values were normalized and analyzed using the *log(inhibitor) vs. normalized response -- Variable slope* regression model. Those analyses used GraphPad Prism 9 Version 9.5.0 (525) for macOS.

K-means clustering analysis was performed to assemble the isolates' phenotypic features. The input data for this analysis was doubling time and the Amb-EC in the promastigote and amastigote stages. The within-cluster sums of squares (Elbow Method) and the average silhouette algorithms were used to determine the number of clusters implemented. These analyses used the *ggplot2*³⁷ and *factoextra*³⁸ packages of R Statistical Software (v4.3.0)³⁹.

Comparative genomics

Reads were mapped to the *L. (V.) braziliensis* MHOM/BR/M2904 reference genome using NGSEP Reads Aligner⁴⁰ with default parameters. Then, the alignments stored in BAM files were sorted and indexed using Picard⁴¹ and were used as input for the Multisample Variants Detector available in NGSEP⁴⁰ with default parameters. The resulting VCF file was filtered to keep only biallelic SNPs, variants with a minor allele frequency (MAF) < 0.01, excluding variants with low qualities (< 40) and with less than 80% of genotyped individuals. NGSEP was also used to generate a neighbor-joining tree (commands DistanceMatrixCalculator and HierarchicalClustering). The tree was visualized in the iTOL web server⁴². Finally, the NGSEP Relative Allele Dosage⁴⁰ function was used to assess the heterozygosity and ploidy of the samples and the reference genome based on relative allele-specific read counts.

The clinical isolates were classified according to their response to AmB for performing an SNP comparative analysis. Comparison was made between AmB tolerant (A28 and A36) vs. AmB-Susceptible (A2, A8, A9, A10, A11, A18, A23, A26, A42, A53 and A66). For previously assessed antimony response³⁵, isolates were classified as SbV most tolerant (A9, A11, A18, A36, A42, A53) vs. less tolerant isolates (A10, A26). The command VCF IntrogressionAnalysis of NGSEP was used to identify the SNPs differentiating groups. The parameters used for this step were -g 95 -d 0.9 -m 0.1 -c. These ensure that 95% of the individuals under consideration are genotyped, a minimum absolute difference in allele frequencies of 0.9, and a maximum MAF within a group of 0.1. A Fisher test on a two-by-two contingency table of allele counts was performed to determine if an SNP significantly differentiated two groups. A Bonferroni correction was applied to control for a false discovery rate due to multiple tests.

Using Samtools⁴³, the normalized sequencing depth was obtained for the 35 chromosomes of all samples, considering the reference genomes *L. (V.) braziliensis* MHOM/BR/75/M2904 and M2903. A comparative matrix of relative ploidy for the 13 isolates was created, and it was visualized as a Heatmap using the *ggplot* and *heatmap2* packages of R Statistical Software v4.3.0 and RStudio v2023.03.1³⁹.

The read depth analysis (option -runRD) of the NGSEP Single Sample Variants Detector⁴⁰ was executed to identify the gene copy number variation. A base ploidy of 1 was set using the option -ploidy. The coordinates of the annotated genes of M2904 were provided as possible CNVs using the option -knownSVs. The remaining options were left with default values. This procedure generated a raw copy number (CN) for each gene on each strain according to the Illumina read depth and normalized it with local GC content and average read depth. The median of the raw CN was calculated for each sample to make predictions consistent with the analysis of global ploidy; then, the values were rescaled to a median consistent with the sample ploidy (three for M2904 and two for the other samples). To select genes with possible CNVs within the clinical isolates, the median and the standard deviation of the scaled CN values were calculated for each gene, excluding M2903 and M2904. Genes with median scaled CN below 2.5 and standard deviation above 0.5 were selected as possible genes with CNVs within the clinical isolates. The rationale for this filtering procedure is that genes with CNVs in a few samples should have a median-scaled CN around the global ploidy because the median is not sensitive to outliers generated by sample-specific CNVs. Conversely, the gene standard deviation should be increased by the presence of samples with abnormally high or low scaled CN values.

Targeted analysis on reported genes

To select specific AmB-resistance reported genes in *Leishmania* spp., a literature search was carried out in the following databases: “PubMed,” “NCBI,” and “Science Direct” using the following terms:

“Trypanosomatids” AND “amphotericin B” AND “resistance” (OR “resistance”)
“Leishmania braziliensis” AND “amphotericin B” AND “resistance” (OR “resistance”).
Leishmania AND “amphotericin B” AND “resistance”.

The literature-referred genes were analyzed in the genome sequences produced by this work, considering gene conservation, identity, single nucleotide polymorphisms (SNPs) within the gene, and CNV. From the SNP variations identified in the VCF file for the 65 genes involved in drug resistance, including nine genes belonging to the ergosterol metabolic pathway. A genotype analysis (GT) was performed filtering them through the command line, retaining only the “missense_variant” type mutations. The filtered genotypes included only GT 0/0, corresponding to a homozygous genotype of reference without alteration in the amino acid, and GT 1/1 represents an alternative homozygous genotype with both altered alleles that cause the change in the amino acid. In addition, it was verified that the variants were located within the coding region of the gene, excluding those present in the UTR regions.

RT-qPCR for genes with increased CN in A28 or A36

Total RNA was extracted from promastigotes in the stationary phase and intracellular amastigotes 24hpi using DirectZol (Zymo) of selected isolates and treated with DNase I. The cDNA used as a qPCR template was synthesized using the high-capacity cDNA reverse transcription kit (Applied Biosystems™, Cat # 4374966). qPCR was performed using SYBR® Select Master Mix (Applied Biosystems™, Cat # 4472897). The qPCR conditions were uracil-DNA glycosylase activation at 50 °C for 2 min, AmpliTaq® DNA Polymerase UP activation at 95 °C for 2 min, denaturing, 40 cycles of 95 °C for 3 s and annealing/extension, and 40 cycles of 60 °C for 30 s.

After assessing qPCR efficiency, gene expression was estimated by calculating the $2^{-\Delta\Delta CT}$. Actin expression was used as a reference gene for expression normalization, and MHOM/BR/75/M2903 was used as a control cell line.

Results

Isolates characterization

Thirteen *L. (V.) braziliensis* clinical isolates obtained from cutaneous lesions of patients suffering CL without response to SbV treatment (Supplementary Table S1)³⁵ were phenotypically characterized by assessing the growth rate as promastigotes and determining the AmB-EC₅₀ as promastigotes and intracellular amastigotes (Table 1).

As detailed in the methods section, the parasite growth curve was generated by daily counting up to 144–168 h (h) of growth (Fig. 1a). Doubling time was estimated using data from time zero up to 72 h to calculate through the exponential growth equation (Fig. 1b). According to their doubling time, about half of the isolates ($n=6$) were grouped as promastigotes with “regular” growth, showing growth rates similar to the reference strain MHOM/BR/75/M2903 (average doubling time of 7.92 ± 0.53 h). The remaining isolates grew slower than the reference strain (F-test, $p < 0.01$), forming three pairs with “delayed” average doubling times of 9.91 ± 0.12 h, 12.98 ± 0.76 h, and 16.31 ± 0.06 h. A23 isolate showed the slowest growth rate of 20.72 h (95% CI; 17.83 to 24.73) (Fig. 1c).

Isolate ID	Doubling time (hours) (95% CI)	Promastigote AmB-EC ₅₀ (μM) (95% CI)	Amastigote AmB-EC ₅₀ (μM) (95% CI)	AmB treatment rounds**
M2903*	8.826 (8.440–9.249)	0.03132 (0.029–0.034)	0.01005 (0.0098–0.01032)	–
A2	8.25 (7.740–8.831)	0.1094 (0.097–0.119)	0.01211 (0.0117–0.0126)	0
A8	9.831 (9.277–10.46)	0.05787 (0.054–0.064)	0.0226 (0.0187–0.0274)	0
A9	12.44 (11.87–13.07)	0.05329 (0.047–0.060)	0.02581 (0.0243–0.0274)	0
A10	7.019 (6.275–7.965)	0.1909 (0.187–0.197)	0.03263 (0.0291–0.0366)	0
A11	16.26 (13.84–19.70)	0.1363 (0.108–0.173)	0.008263 (0.0035–0.0146)	0
A18	7.779 (7.266–8.370)	0.04701 (0.045–0.048)	0.01488 (0.0139–0.0159)	0
A23	20.72 (17.83–24.73)	0.01876 (0.013–0.023)	0.007782 (0.0071–0.0329)	0
A26	13.52 (10.97–17.63)	0.04361 (0.038–0.054)	0.007306 (0.0062–0.0085)	0
A28	7.706 (7.053–8.492)	0.09162 (0.086–0.094)	0.2787 (0.2610–0.2985)	2
A36	16.35 (15.35–17.49)	0.163 (0.140–0.167)	0.1689 (0.1371–0.2154)	0
A42	9.995 (9.690–10.32)	0.08885 (0.062–0.108)	0.01816 (0.0176–0.0188)	0
A53	8.385 (7.589–9.368)	0.1136 (0.091–0.138)	0.01365 (0.0117–0.0158)	0
A66	8.385 (7.589–9.368)	0.2254 (0.197–0.251)	0.001374 (1.9e-005–0.0144)	3

Table 1. Phenotypic features of clinical isolates. *Reference Strain. **Number of completed AmB treatment cycles administrated to the patient before the parasite was isolated.

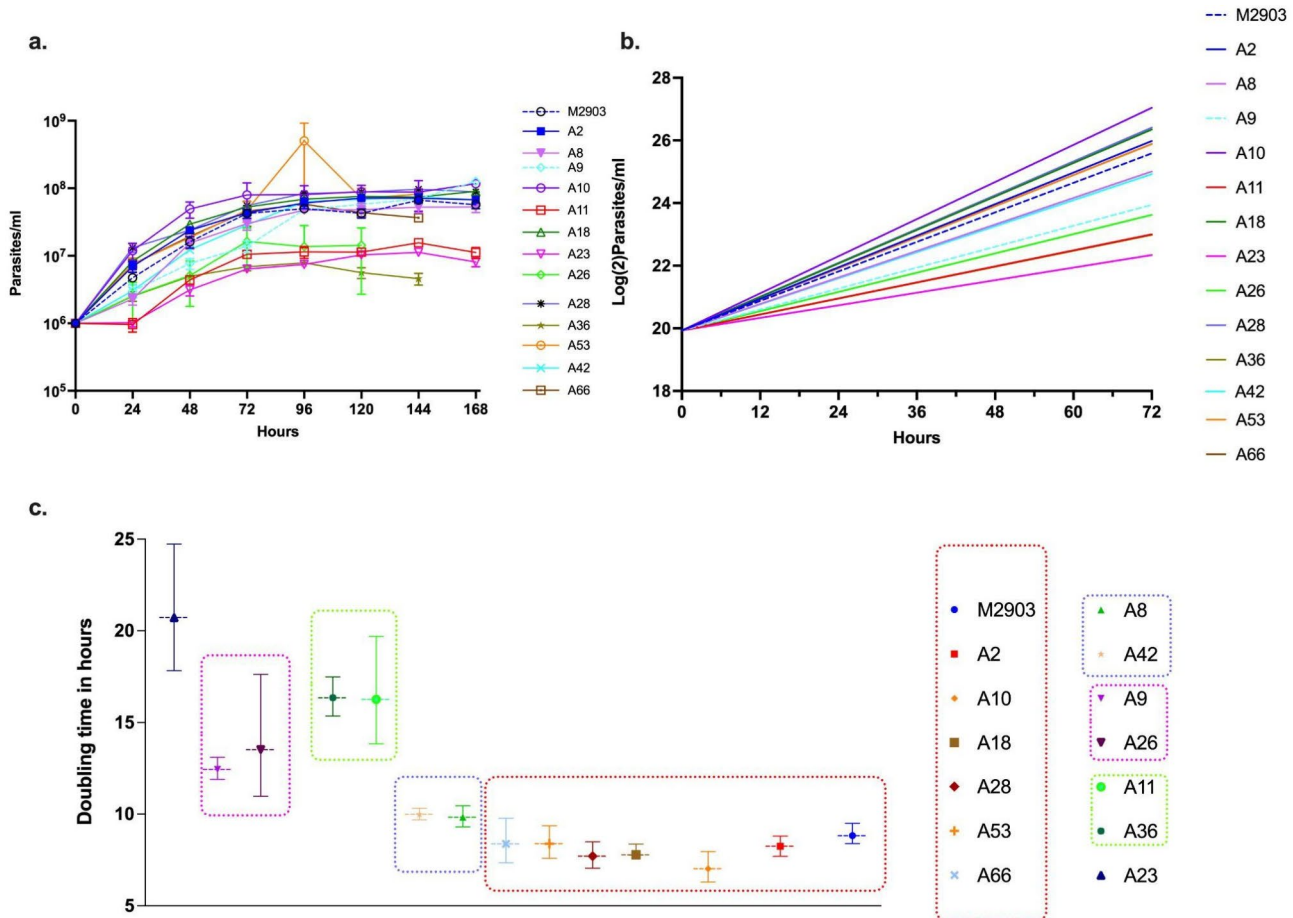


Fig. 1. Clinical isolates growth characterization. The isolates growth curve in hours (a); growth curve expressed as \log_2 (b) and estimated doubling time in hours (c). M2903 corresponds to the MHOM/BR/75/M2903 reference strain. The colored dotted lines group the isolates showing identical doubling time. Doubling time between groups presents statistically significant differences (F-test, $p < 0.01$). Growth data correspond with the average of two biological replicates (counted by the Newbauer chamber, with three counting replicas) and the error bars presented in (A) correspond with the SD for the raw counting. The doubling time values are presented in (C) were estimated using the “exponential growth with log population” function using GraphPad Prism 9 Version 9.5.0 (525) for macOS. The error bars in this figure correspond with the 95% CI reported by the program.

Parasites clustering according to in vitro growth and AmB susceptibility

The AmB susceptibility was assessed for both parasite stages of the 13 clinical isolates and the reference strain. For the promastigote stage, the AmB- EC_{50} was evaluated by the fluorescence-based resazurin assay and calculated in promastigotes exposed to AmB for 48 h. The promastigote AmB- EC_{50} ranged from $0.0178 \mu\text{M}$ to $0.225 \mu\text{M}$ (Fig. 2a; Table 1 and Supplementary Figure S1). At the promastigote stage, isolate A66 exhibited the highest tolerance to AmB. Its EC_{50} was 4.82 times higher than that of the reference strain and 12.63 times higher than that of the most susceptible isolate, A23.

As detailed in the methods section, the AmB susceptibility in U-937 intracellular amastigotes was assessed through multiplex RT-qPCR after 96 h of AmB treatment. For the intracellular amastigote stage, the AmB- EC_{50} ranges from $0.0057 \mu\text{M}$ to $0.279 \mu\text{M}$ (Fig. 2b; Table 1 and Supplementary Figure S2). At this stage, two clinical isolates exhibited the highest AmB- EC_{50} value: isolate A28 and isolate A36. The AmB- EC_{50} for isolate A28 was 25.7 times higher than that of the reference strain and 49 times higher than that of the most susceptible isolate, A66. Likewise, the AmB- EC_{50} for isolate A36 was 15.6 times that of the reference strain and 29.7 times that of isolate A66. Additionally, all isolates, except A28 and A36, presented higher AmB- EC_{50} values in the promastigote life stage compared to the intracellular amastigote stage (Fig. 2c; Table 1).

Regarding the potential correlation between the promastigotes' doubling time and their AmB susceptibility and given that both sets of data showed a normal distribution, a Pearson correlation coefficient was performed, showing no significative value ($r, -0.2546$; 95% CI, -0.6917 to 0.3191); the amastigote AmB susceptibility values had no normal distribution, and the no parametric Spearman test evidenced that they are not correlated with the promastigote doubling time ($r, -0.3014$; 95% CI, -0.7257 to 0.2889).

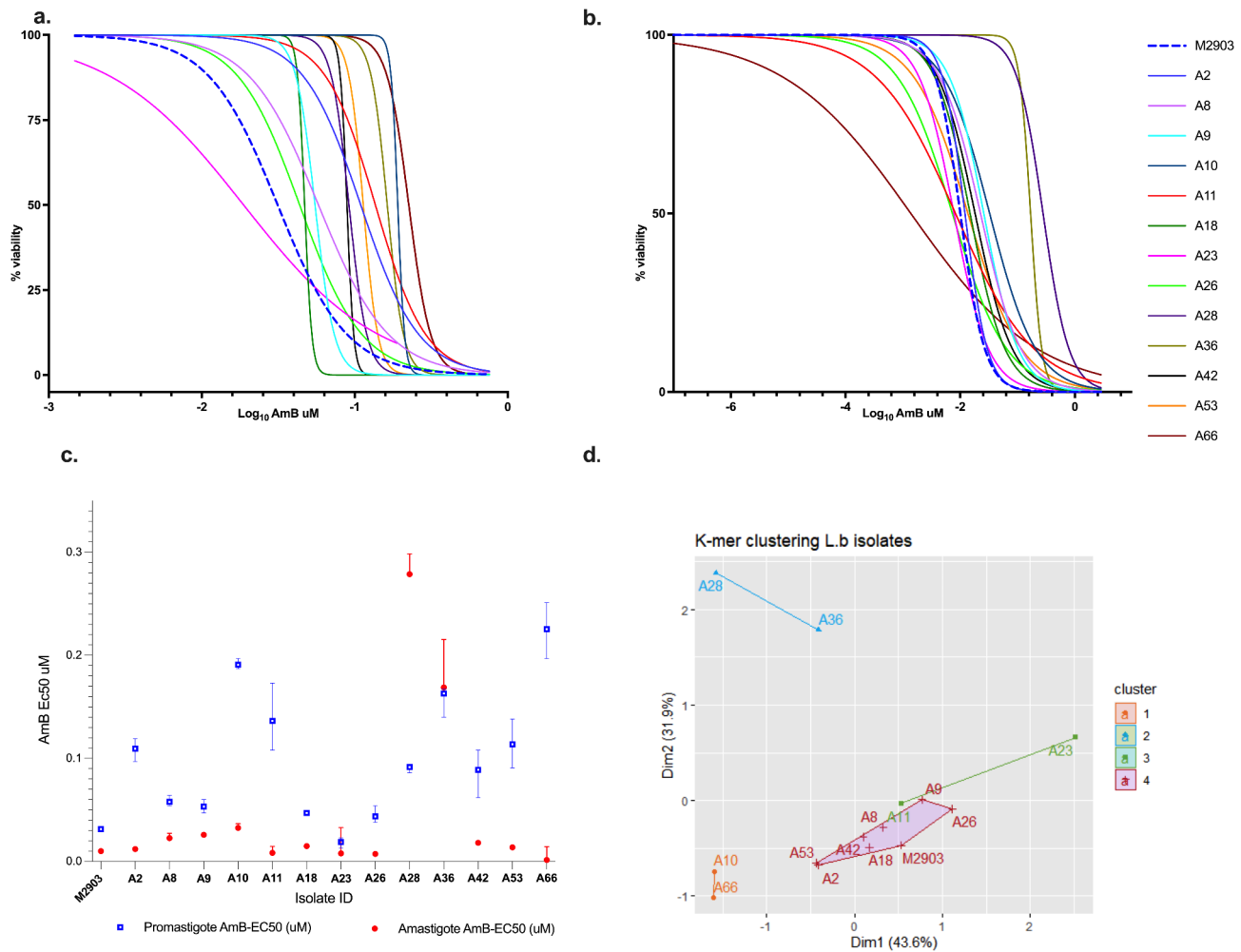


Fig. 2. Clinical isolate clusters regarding growth rate and AmB susceptibility. Nonlinear regression with a variable slope of Log of AmB concentration vs. parasite survival (normalized response) in promastigotes (**a**) and amastigotes (**b**) for each isolate. A scatter graph presents the clinical isolate AmB EC₅₀ by life stage (**c**). Clusters were produced using the optimal number of clusters analysis with the K-means clustering using 4 clusters (**d**). AmB susceptibility data for the promastigote stage were generated from four technical replicas and as an amastigote from three experimental replicas. The EC₅₀ was estimated using log(inhibitor) vs. normalized response -- Variable slope regression model, and the error bars presented in **c** correspond with the values of 95% CI estimated by the program for each EC₅₀ calculated.

A cluster analysis was performed to group the clinical isolates according to their phenotypic features: growth rate and AmB- susceptibility (AmB-EC₅₀) as promastigote and amastigote. Due to their shared phenotypic features, 4 clusters were identified (Fig. 2d). Cluster 1 (orange) was composed of A10 and A66 isolates. Those isolates have the highest AmB-EC₅₀ in the promastigote stage, and both are above the doubling time median. Cluster 2 (blue) was composed of A28 and A36 isolates. Those isolates have the highest AmB-EC₅₀ in the amastigote stage, and both are over the EC₅₀ median in the promastigote stage. Cluster 3 (green) was composed of A11 and A23 isolates. The doubling time is the primary explicative variable for this cluster, given that these isolates present the second longest doubling time. Besides, both have a similar AmB-EC₅₀ in the amastigote stage, being among the isolates having the lowest tolerance to the drug. Finally, Cluster 4 (red) comprised A2, A8, A9, A18, A26, A42, and A53 isolates and the reference strain M2903. This last group of isolates could be considered the standard group, presenting average doubling time and AmB-EC₅₀.

Genomic characterization of the isolates

Illumina whole genome sequencing (WGS) was performed for the characterized isolates. Following a variant detection and genotyping pipeline using the *L. (V.) braziliensis* MHOM/BR/75/M2904 (M2904) assembly as a reference, a genomic variation database of 332,321 SNPs was built up. The database included 15 genomes [13 clinical isolates and two reference strains: (*L. (V.) braziliensis* MHOM/BR/75/M2904 and M2903)] with 1.24% missing data. A neighbor-joining clustering based on this genomic information shows that although the clinical isolates grouped separately from the reference strains (Fig. 3A), they did not group according to their AmB tolerance profile or growth curves (Fig. 2D). The average number of heterozygous SNPs for all clinical

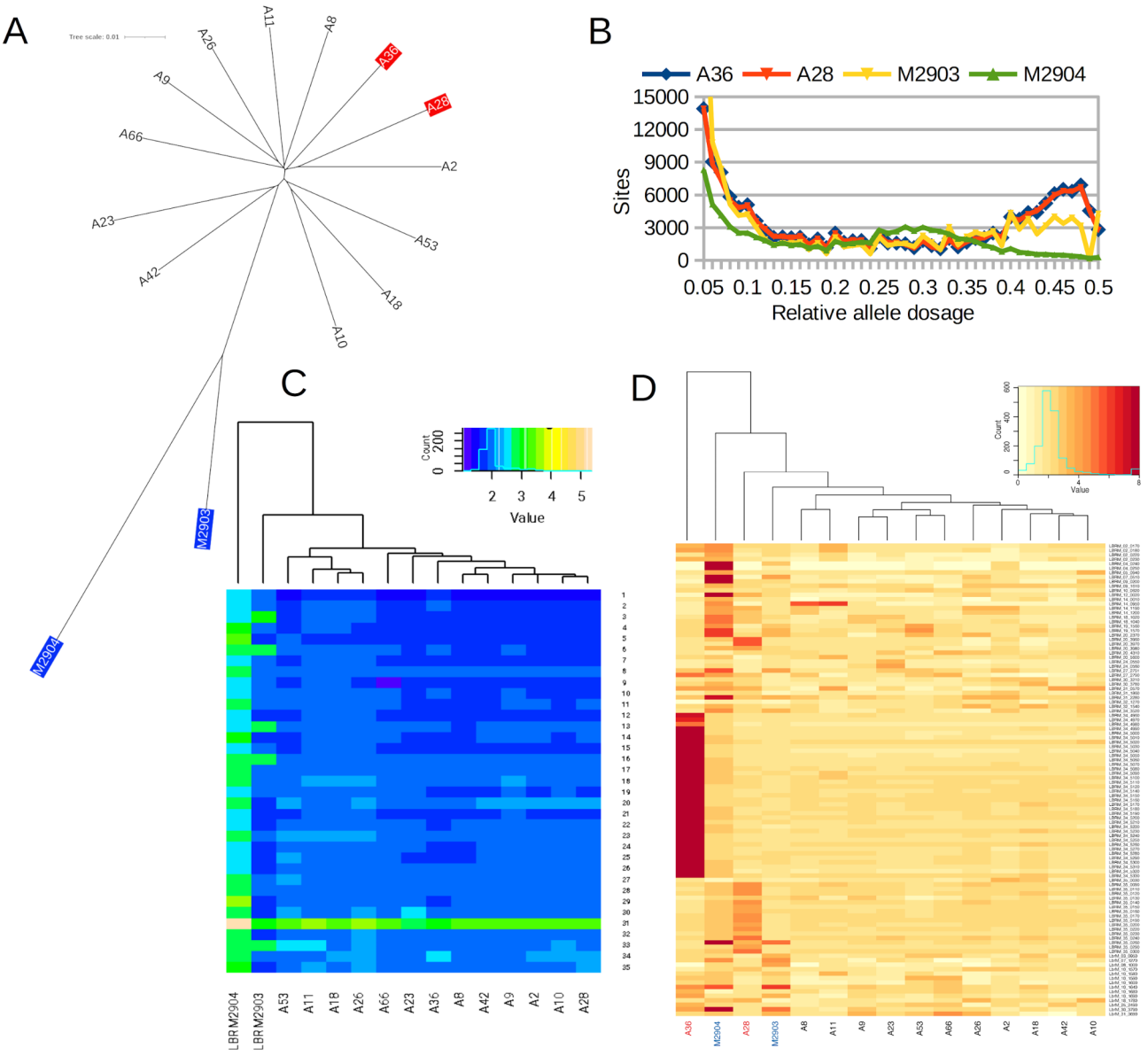


Fig. 3. Analysis of genomic variability among clinical isolates (A). Neighbor-joining clustering of the isolates based on biallelic SNPs. Blue labels correspond to the reference genomes, and red labels correspond to the AmB-tolerant isolates. (B) Allele dosage distribution for genomic locations having more than one allele represented in the aligned reads. (C) Chromosome ploidy variation among the isolates. (D) Predicted number of copies for the 106 genes with low (below 2.5) median CN values and high (above 0.5) standard deviation.

isolates was 61,123, corresponding to about 19% of the genotyped SNPs and a density of 1 SNP for each 525 bp (Supplementary Table S2). The reference strains present 34,768 (M2904) and 48,943 (M2903) heterozygous SNPs. The graph of allele dosages related to this heterozygosity suggests an overall ploidy of two, except for M2904, which shows a curve consistent with a ploidy of three (Fig. 3B and Supplementary Figure S3). However, read depth per chromosome indicates the presence of aneuploidies in about half of the genome of M2904, six chromosomes of M2903, and chromosome 31 of all isolates (Fig. 3C).

The comparative SNP analysis between the genome of the AmB-tolerant isolates (A36 and A28) vs. the rest of the isolates (Supplementary Table S3.A) shows 32 SNPs that differentiate the AmB-tolerant isolates from the other isolates. They were located close to or within fifteen genes. Missense variants differentiating A28 and A36 were present on one gene (LBRM.23.1680) and one pseudogene (LBRM.33.3340). Regarding significance, although at first glance, the p-values look significant (Supplementary Table S3.A, column AA), they would not be significant in a normal GWAS after the Bonferroni correction for multiple testing. In this case, the Bonferroni cutoff would be 0.05 divided by the total statistical tests ($n=332,321$). This would give a cutoff of 1.5×10^{-7} . A similar interpretation was made for the same analysis results between the previously characterized most SbV-tolerant isolates (A9, A11, A18, A36, A42, and A53) vs. the most susceptible ones (A10 and A26³⁵). Only 21 variants differentiate SbV most tolerant from less tolerant groups. The variants are located within or close to 13

genes, and four are missense within genes encoding for hypothetical proteins LBRM.08.0460, LBRM.21.0590, LBRM.34.4270, and the gene LBRM.35.6540 encoding for a putative flagellum transition zone component (Supplementary Table S3.B).

We estimated the local copy number for each gene (CN) within each isolate from the normalized average read depth. Consistent with the ploidy analysis, 71.6% of the CN values were between 1.5 and 2.5 for the diploid clinical isolates, and this percentage increases to 88.8% if the range is widened between 1 and 3. A positive trend can be observed by plotting the average and the variance of CN values per gene within the clinical isolates (Supplementary Figure S4). From this analysis, 106 genes were identified, presenting low (below 2.5) median CN values and relatively high (standard deviation above 0.5) CN variability between clinical isolates (Fig. 3D and Supplementary Table S4). Although no common genes are duplicated exclusively in A28 and A36, fifty-seven out of the 106 genes (53.7%) show high CN exclusively in one of these genomes (Supplementary Table S4). For this reason, a principal component analysis of the isolates based on CN values for this group of 106 genes separates the isolates A28 and A36 from the others (Supplementary Figure S5).

Available information on orthologues in *Leishmania* spp. of the selected 106 genes suggests a potential association for some of them with experimentally induced resistance to SbV or AmB in *L. (L.) infantum*, *L. (L.) tropica*, and *L. (L.) donovani* (Supplementary Table S5). For instance, the orthologue in *L. (L.) infantum* of the gene LbrM.20.2370 (amastin-like, putative) was upregulated in the antimony-activated-translatome of antimony-resistant promastigotes of *L. (L.) tropica*⁴⁴. Other genes with increased CN in the clinical isolates whose orthologues showed increased translation in antimony-resistant *L. (L.) tropica* were LbrM.19.1560 (glycerol uptake protein, putative), LbrM.10.0620 (map kinase 3, putative, mitogen-activated protein kinase 3, putative), and LbrM.20.4310 (amastin-like, putative)⁴⁴. The *L. (L.) donovani* orthologue of LbrM.20.4310 was also upregulated in AmB-resistant and antimony-resistant cell lines⁴⁵. However, the genes mentioned above did not present marked CNV or were unique for the AmB-tolerant isolates in this study. From the group of genes with high CN values in several isolates, it is worth highlighting a galactosyl transferase located in chromosome 31. Orthology information regarding other genome assemblies suggests that this gene is unique to *L. (V.) braziliensis* (Supplementary Figure S6).

Thirty-nine genes (thirty-eight on chromosome 34 and one on chromosome 27) present high CN values exclusively in isolate A36 (Supplementary Table 4). The genes on chromosome 34 are embedded in a single 150 kb subtelomeric region, corresponding with the previously described LD1 locus⁴⁶. Three genes (LbrM.34.5330, LbrM.34.5150, and LbrM.34.5090) that were exclusively duplicated in the A36 isolate were previously reported as associated with AmB- or antimony-resistance⁴⁵ (Supplementary Table 5); the orthologue of the putative biotin transporter (LbrM.34.5090) also appears with increased CN in experimentally induced AmB-resistant *L. (L.) mexicana*²⁶. In addition, there is a gene encoding for a hypothetical protein located in chromosome 27 that is deleted in A36 and a translation initiation factor located on chromosome 12 that is partially deleted in this same isolate (Supplementary Table 4).

For the A28 isolate, eighteen genes present high CN values exclusively in this isolate (three on chromosome 20 and fifteen on chromosome 35 (Supplementary Table 4). The genes in chromosome 20 are an NADH ubiquinone oxidoreductase subunit (ESSS subunit, putative), a quinonoid dihydropteridine reductase, and the 20s proteasome beta 7 subunit (putative). Synteny analysis shows that the region where these genes are located presents substantial rearrangements, particularly in *L. (L.) major* genomes. *L. (L.) mexicana* (MHOM/GT/2001) orthologues of the three genes mentioned above were also identified with increased copy number in experimentally induced AmB-resistant parasites²⁶ (Supplementary Table 5).

A66 is an isolate that is highly tolerant as a promastigote but not as an amastigote. This isolate presents increased CN in genes LbrM.10.1590 and LbrM.31.3690, which encode GP63 (leishmanolysin) and a conserved hypothetical protein, respectively. This isolate also shows the maximal reduction in CN for genes LbrM.02.0220 and LbrM.07.1270, which correspond to phosphoglycan beta 1,3 galactosyltransferase and a putative glycosyl transferase, respectively.

Analysis of known genes associated with AmB tolerance in *Leishmania* spp.

We further investigated variation (SNPs, indels, and CN values) for 65 genes previously associated with resistance to antileishmanials (Supplementary Table 6). Forty of those genes present missense variants in some of the clinical isolates, and none correspond with substitutions previously reported to be associated with AmB- resistance (Supplementary Table 6.B). However, the gene identified as LbrM.30.2210 (on a putative phospholipid-translocating P-type ATPase (flippase)) could be interesting because it presents an A28-unique missense variant producing S226P substitution on the P-type ATPase domain. This protein was identified in the genome-scale orthology-based chemogenomic profiling approach of the *T. brucei* RNA interference (RNAi) library to be potentially associated with cross-resistance between miltefosine and amphotericin B⁴⁷.

AmB-tolerance-associated loci, previously identified in a gain-of-function screen on the *Leishmania* (*L. infantum*) genome⁴⁸, were analyzed in the genomes of the two *L. (V.) braziliensis* AmB-tolerant clinical isolates. However, none of the previously identified loci exhibited CNV in the genomes of the tolerant clinical isolates in the current study (Supplementary Table 6.D).

RT-qPCR analysis of genes encompassed in duplicated regions of A28 or A36

To assess the concurrence between genomic duplications and their correspondent mRNA levels in promastigotes and intracellular amastigotes of the AmB-tolerant isolates, an RT-qPCR of randomly selected genes embedded in the duplicated regions of A28 and A36 was performed for promastigotes and intracellular amastigotes, using M2903 as a reference cell line. The relative expression of selected genes normalized to the expression of the genes in M2903 shows that the genomic duplication (Fig. 4A) does not match mRNA levels (Fig. 4B). However, the

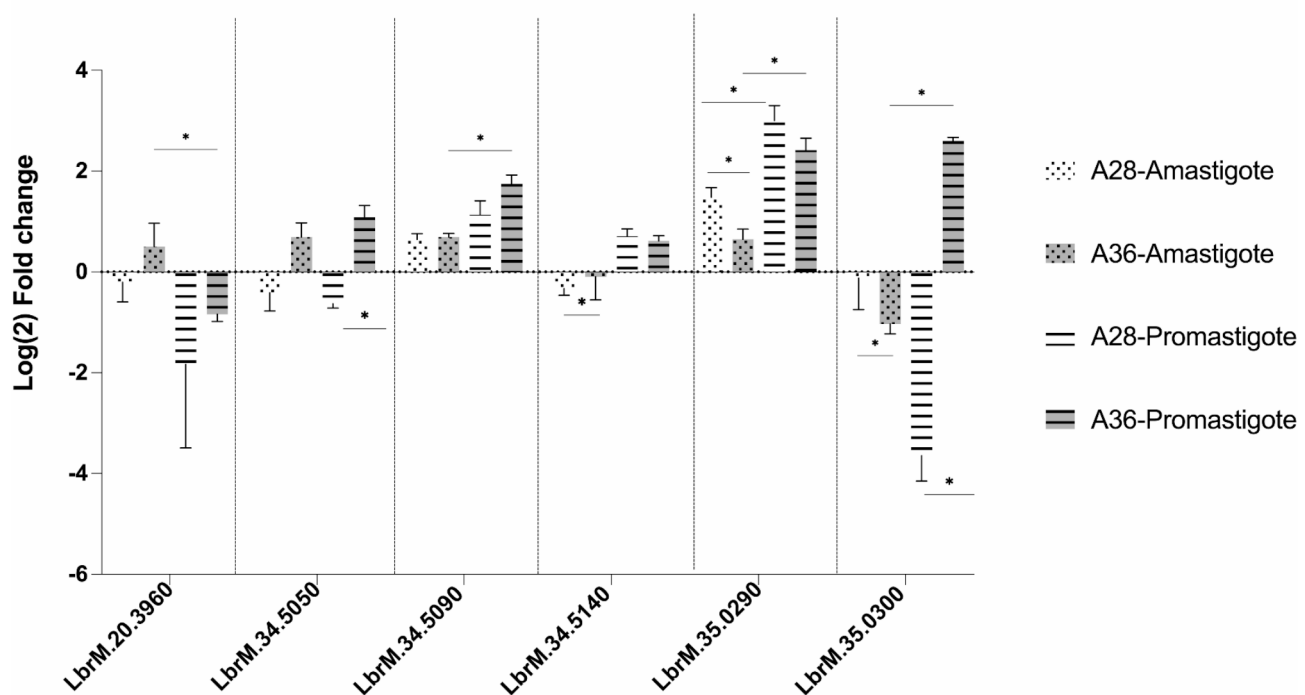
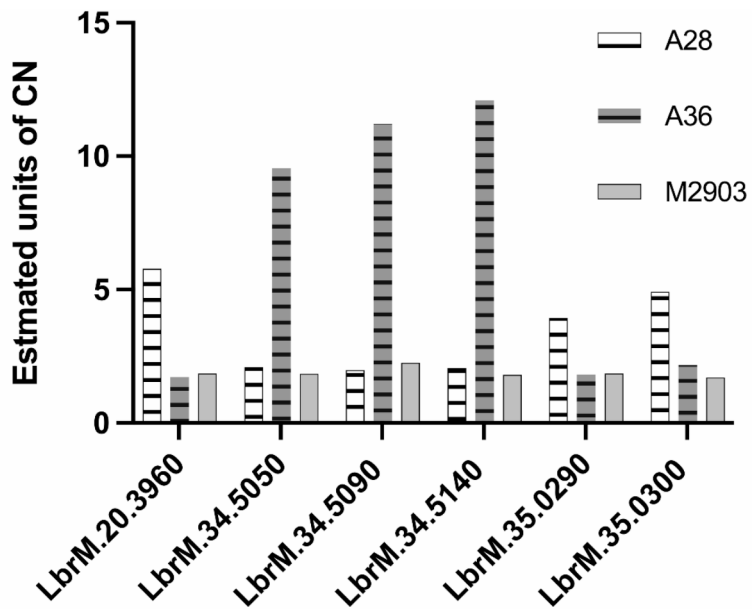


Fig. 4. Expression analysis of randomly selected genes from duplicated genomic regions on chromosomes 20, 34, and 35 in clinical isolates with higher tolerance to AmB (A28 and A36). (A) Estimated copy number of genes per genome for each isolate. (B) Levels of mRNA of randomly selected genes embedded in duplicated regions were evaluated for each life cycle stage by RT-qPCR. Expression values are presented as the Log2 of the $2^{(\Delta\Delta CT)}$ to estimate the fold change regarding M2903. The gene encoding for actin was used as the normalizer.

genes encoding for the bipterin transporter [(putative), LbrM.34.5090] and SET domain protein [(putative), LbrM.35.0290] were consistently upregulated for both life stages of the clinical isolates.

From our list of 106 genes with increased CN (Supplementary Table 4), we ran a search in TriTrypDB looking for genes that present upregulation with a fold change >2 in the amastigote stage vs. promastigote, using the data reported by Ruy, 2019⁴⁹. This analysis identified genes with increased CN exclusively in A28 (the

NADH: ubiquinone oxidoreductase, ESSS subunit, LbrM.20.3960) and A36 (conserved hypothetical protein, LbrM.34.5150).

Discussion

The present work intended to assess the distinctive genomic features of the *L. (V.) braziliensis* isolates with the highest in vitro AmB tolerance among a set of phenotypically characterized isolates. The parasites were derived from CL lesions of patients who did not respond to SbV treatment³⁵ and some of whom did not respond to AmB treatment (Supplementary Table S1).

The phenotypic assessment covered promastigote' growth and their sensitivity to AmB along with the sensitivity of in vitro macrophage-resident amastigotes to AmB. Cluster analysis regarding their phenotypic features assembled four main groups: two groups correspond to isolates that showed high tolerance to AmB, one as promastigotes (A10 and A66) and the other as amastigotes (A36 and A28). Therefore, the remaining nine isolates forming the other two groups corresponded to intermediate and low AmB tolerance at both stages and were considered AmB-susceptible isolates (Fig. 2; Table 1).

It has been observed that antimony-tolerant clinical isolates of *L. (L.) donovani* present an overall increased fitness, reaching stationary phase at higher promastigote density than the susceptible parasites⁵⁰. Similar findings have been reported in antimony-tolerant *L. (V.) guyanensis* and AmB-resistant *L. (Mundinia) martinicensis* clinical isolates, which show different growth patterns from susceptible ones^{51,52}. The parasites' duplication time observed in this study indicated that three (A10, A28, A66) out of four AmB-tolerant isolates presented a "regular" growth rate, and one AmB-tolerant (A36) showed a delayed growth (Figs. 1 and 2D; Table 1). Furthermore, in the group of "regular" growth, there are also three AmB-susceptible isolates, suggesting the in vitro AmB response observed in these isolates is unrelated to the promastigotes' doubling time.

Regarding the growth rate in promastigotes, isolate A36 carries the LD1 locus previously associated with increased cell growth in the presence of folate, biotin, or tetrahydrobiotin (BH4)⁵³. Here, the promastigotes were grown in Schneider's medium without biotin or folate, which could explain the different results (Fig. 1).

Assessment of the AmB susceptibility in promastigotes shows two isolates with the highest tolerance to the drug (Fig. 2A); one of them (A66) comes from a patient who had received three complete AmB treatments without response and whose lesion was in the ear helix (Supplementary Table S1), a tissue microenvironment with presumably low bioavailability for systemic drugs. Interestingly, this isolate was the most susceptible in the amastigote stage (Fig. 2B and C). At the genomic level, A66 showed a heterozygous polymorphism in a gene encoding a hypothetical protein (LbrM.23.1680) that contains predicted transmembrane domains and for which the homozygous variant is associated exclusively with the isolates most tolerant to AmB (A28 and A36) (Supplementary Table S3), making this SNP distinctive of the AmB-tolerant isolates in the present study. A66 also showed a decreased copy number (CN) of genes associated with glycosylation and galactosylation transferase activity (see Supplementary Table S4). One such gene is the phosphoglycan beta 1,3 galactosyltransferase, for which mRNA levels were found to be distinctively reduced in a human isolate of *L. (L.) major*, recognized for its low infectivity compared to a highly infective *L. (L.) major* human isolate⁵⁴. Therefore, the low tolerance observed in the A66 intracellular amastigotes (which are highly tolerant as promastigotes) may arise from the selection process during in vitro infection. This selection might lead to tolerant promastigotes having a lower likelihood of becoming intracellular, or their growth as amastigotes could be impaired. This would indicate that the mechanisms behind tolerance in A66 promastigotes differ from those in the A28 isolate, which requires further investigation.

The decision of the appropriate life stage of the parasite to assess the drug response profile is a matter of debate. Approaches using promastigotes have revealed resistance mechanisms with significant clinical and epidemiological implications^{16,20,55}. However, systematic assays comparing the performance of promastigote cultures vs. intracellular amastigote tests for evaluating the effectiveness of existing drugs in leishmaniasis treatment suggest that the second setting showed a better correlation with the clinical outcome of therapy⁵⁶. Nevertheless, the genomic analysis presented here found changes in isolates that had the highest AmB tolerance as intracellular amastigotes (A28 and A36 (Fig. 3B and D)) vs. the rest of the isolates but also on an isolate that presents the highest tolerance to AmB as promastigote but the most significant susceptibility as intracellular amastigotes (A66).

The overall ploidy analysis and the SNP variability analysis did not show any large structural difference between the genomes of AmB most tolerant isolates and those of the AmB less tolerant isolates. The genomes of A28 and A36 present CNV in genes previously associated with AmB tolerance (Supplementary Table 5). Additionally, the SNP analysis exposed a substitution (P177S) distinctive of the A28, A36, and A66 on a conserved hypothetical protein presenting transmembrane domains (LbrM.23.1680). Also the SNP analysis revealed a mutation given by S226P substitution on the P-type ATPase domain of a flippase gene (LbrM.30.2210), exclusively in the most AmB-tolerant isolate (A28). Losses and mutations in the flippase responsible for miltefosine transport have previously been linked to resistance to AmB in *L. (L.) mexicana* and *L. (L.) infantum* promastigotes^{24,26,34}. The flippase gene identified in this study does not correspond to the known miltefosine transporter; rather, it aligns with a gene whose *T. brucei* orthologue has been associated with cross-resistance between AmB and miltefosine in an RNA interference library⁴⁷. Therefore, the situation is complex, and further investigations into the membrane rearrangements in response to both drugs in amastigotes and promastigotes are required.

In *L. (L.) infantum*, genomic analysis of field isolates categorized by their miltefosine treatment outcomes led to the identification of a miltefosine sensitivity locus (MSL)⁵⁷. This locus was then experimentally evaluated to investigate the key genes involved in the response to miltefosine⁵⁸. Similarly, the current study has compiled a list of candidate genes for further functional experiments to examine the relationship between these genomic variations and the observed tolerance to amphotericin B (AmB).

When comparing the AmB response between A28 and A36, it is clear that A36 is tolerant in both stages, promastigote and amastigote, while A28 is only tolerant as amastigote (Fig. 2C). The LD1 locus, the region that is duplicated in A36, encompasses genes such as the biotin transporter (BT1). Despite BT1 not being directly involved in antileishmanial resistance, the fact that the parasite is a pteridine auxotroph and the pteridine derivates counteract the oxidative stress and improve the parasite intracellular survival⁵⁹, increasing intake of unconjugated pteridines could provide the parasite with an oxidative stress tolerance generic mechanism selected under oxidative injuries. This assumption aligns with: (1) the upregulation of BT1 observed in antimony-resistant *L. (L.) donovani*⁴⁵, (2) the amplification of the orthologue gene observed in AmB-resistance *L. (L.) mexicana*²⁶, (3) the increased levels of the BT1 mRNA (LbrM.34.5090) in A28 and A36 (Fig. 4B), and (4) the increased CN in A28 for the gene encoding for quinonoid dihydropteridine reductase (LbrM.20.3970), the enzyme responsible for the reduction of dihydrobiopterin (qBH2) to BH4, a gene that is also amplified in AmB-resistance *L. (L.) mexicana*²⁶ (Supplementary Table 5). The present study, limited to genomic analysis, did not detect other genes involved in this detoxification pathway, probably because CNV is only one of the adaptive responses used by the parasite⁶⁰.

Another gene of interest, with increased CN in A28, corresponds with the gene encoding for dolichol phosphate-mannose synthase (LbrM.35.0300). The product of this gene is an endoplasmic reticulum associated enzyme that forms dolichol phosphate-Man (Dol-P-Man), a critical Man derivative used for glycosylation reactions involved in the synthesis of glycosylphosphatidylinositol (GPI)-anchored glycoproteins, a GPI-anchored lipophosphoglycan, and a class of free GPI glycolipids⁶¹. Contrary to expectations, in the preliminary expression analysis performed in this study, this gene showed high mRNA levels only in promastigotes of A36. However, this gene remains of interest given that its impairment in *Saccharomyces cerevisiae* increases the yeast's sensitivity to AmB⁶², and other genes that share metabolic pathways with it have been implicated in antimony resistance and parasite virulence in *Leishmania* spp^{63,64}.

In summary, isolates A66 and A28 were exposed to AmB in vivo, and the observed differences in their in vitro responses to AmB suggest that the mechanisms underlying their in vitro tolerance differ and may not be easily identified using an exclusively genomic approach. In contrast, isolate A36, which was not previously exposed to AmB, shows similar in vitro responses in both life stages. The lack of shared genomic features among these isolates, apart from substitution in the hypothetical protein LbrM.23.1680 and their varying responses based on life cycle stages, indicates an underlying complexity in the AmB refractoriness. Further studies investigating the genes identified in this study may uncover new determinants that influence the AmB response in *Leishmania*.

Data availability

The data used in this study is available at the NCBI sequence read archive (SRA) database (<https://www.ncbi.nlm.nih.gov/sra>) with bioproject accession number PRJNA1095027.

Received: 23 October 2024; Accepted: 1 April 2025

Published online: 15 April 2025

References

1. World Health Organization. Control of the leishmaniasis. *World Health Organ. Tech. Rep. Ser.* **949**, 67–71 (2010).
2. Peters, W. & Killick-Kendrick, R. *The Leishmaniasis in Biology and Medicine. Vol I. Biology and Epidemiology*44–47 (1987).
3. Reithinger, R. et al. Cutaneous leishmaniasis. *Lancet Infect. Dis.* **7** (9), 581–596. [https://doi.org/10.1016/S1473-3099\(07\)70209-8](https://doi.org/10.1016/S1473-3099(07)70209-8) (2007).
4. Tuon, F. F. et al. Treatment of new world cutaneous leishmaniasis—a systematic review with a meta-analysis. *Int. J. Dermatol.* **47** (2), 109–124. <https://doi.org/10.1111/j.1365-4632.2008.03417.x> (2008).
5. Perry, M. R. et al. Arsenic exposure and outcomes of antimonial treatment in visceral leishmaniasis patients in Bihar, India: a retrospective cohort study. *PLoS Negl. Trop. Dis.* **9** (3), e0003518 (2015).
6. Hadighi, R. et al. Unresponsiveness to glucantime treatment in Iranian cutaneous leishmaniasis due to drug-resistant leishmania tropica parasites. *PLoS Med.* **3** (5), e162. <https://doi.org/10.1371/journal.pmed.0030162> (2006).
7. Sundar, S. & Singh, A. Chemotherapeutics of visceral leishmaniasis: present and future developments. *Parasitology* **145** (4), 481–489. <https://doi.org/10.1017/S0031182017002116> (2018).
8. Wijnant, G. J. et al. Relation between skin pharmacokinetics and efficacy in ambrisome treatment of murine cutaneous leishmaniasis. *Antimicrob. Agents Chemother.* **62** (3), e02009–e02017. <https://doi.org/10.1128/AAC.02009-17> (2018).
9. Motta, J. O. & Sampaio, R. N. A pilot study comparing low-dose liposomal amphotericin B with N-methyl glucamine to treat American cutaneous leishmaniasis. *J. Eur. Acad. Dermatol. Venereol.* **26**, 331–335 (2012).
10. Solomon, M., Pavlitzky, F., Barzilai, A. & Schwartz, E. Liposomal amphotericin B in comparison to sodium stibogluconate for leishmania brasiliensis cutaneous leishmaniasis in travelers. *J. Am. Acad. Dermatol.* **68**, 284–289 (2013).
11. Rodriguez Galvis, M. C., Perez Franco, J. E., Casas Vargas, M. Y. & Rubiano, O. Effectiveness and safety of amphotericin B deoxycholate, amphotericin B colloidal dispersion, and liposomal amphotericin B as third-line treatments for cutaneous and mucocutaneous leishmaniasis: A retrospective study. *Am. J. Trop. Med. Hyg.* **102**, 274–279 (2020).
12. Hadighi, R. et al. Glucantime-resistant leishmania tropica isolated from Iranian patients with cutaneous leishmaniasis are sensitive to alternative antileishmania drugs. *Parasitol. Res.* **101**, 1319–1322. <https://doi.org/10.1007/s00436-007-0638-0> (2007).
13. Lira, R. et al. Evidence that the high incidence of treatment failures in Indian kala-azar is due to the emergence of antimony-resistant strains of leishmania donovani. *J. Infect. Dis.* **180** (2), 564–567. <https://doi.org/10.1086/314896> (1999).
14. Jedd, F. et al. Heterogeneity of molecular resistance patterns in antimony-resistant field isolates of leishmania species from the Western mediterranean area. *Antimicrob. Agents Chemother.* **58** (8), 4866–4874. <https://doi.org/10.1128/AAC.02521-13> (2014).
15. Rugani, J. N., Gontijo, C. M. F., Frézard, F., Soares, R. P. & Monte-Neto R.L.D. Antimony resistance in leishmania (Viannia) brasiliensis clinical isolates from atypical lesions associated with increased ARM56/ARM58 transcripts and reduced drug uptake. *Mem. Inst. Oswaldo Cruz.* **114**, e190111. <https://doi.org/10.1590/0074-02760190111> (2019).
16. Faral-Tello, P., Greif, G., Satragno, D., Basmajian, Y. & Robello, C. Leishmania infantum isolates exhibit high infectivity and reduced susceptibility to amphotericin B. *RSC Med. Chem.* **11** (8), 913–918. <https://doi.org/10.1039/d0md00073f> (2020).
17. De Moura, T. R. et al. Cross-resistance of leishmania infantum isolates to nitric oxide from patients refractory to antimony treatment, and greater tolerance to antileishmanial responses by macrophages. *Parasitol. Res.* **115** (2), 713–721. <https://doi.org/10.1007/s00436-015-4793-4> (2016).

18. Purkait, B. et al. Mechanism of amphotericin B resistance in clinical isolates of leishmania donovani. *Antimicrob. Agents Chemother.* **56** (2), 031–41. <https://doi.org/10.1128/AAC.00030-11> (2012).
19. Kumar, D., Kulshrestha, A., Singh, R. & Salotra, P. In vitro susceptibility of field isolates of leishmania donovani to miltefosine and amphotericin B: correlation with sodium antimony gluconate susceptibility and implications for treatment in areas of endemicity. *Antimicrob. Agents Chemother.* **53** (2), 835–838. <https://doi.org/10.1128/AAC.01233-08> (2009).
20. Equbal, A. et al. Stage-dependent expression and up-regulation of trypanothione synthetase in amphotericin B resistant leishmania donovani. *PLoS One.* **9** (6), e97600. <https://doi.org/10.1371/journal.pone.0097600> (2014).
21. Ghosh, S. et al. A novel bioimpedance-based detection of Miltefosine susceptibility among clinical Leishmania donovani isolates of the Indian subcontinent exhibiting resistance to multiple drugs. *Front Cell Infect Microbiol.* 768830. <https://doi.org/10.3389/fcmb.2021.768830> (2021).
22. Franco-Muñoz, C., Manjarrés-Estremor, M. & Ovalle-Bracho, C. Intraspecies differences in natural susceptibility to amphotericin B of clinical isolates of leishmania subgenus Viannia. *PLoS One.* **13** (4), e0196247. <https://doi.org/10.1371/journal.pone.0196247> (2018).
23. Ponte-Sucre, A. et al. Drug resistance and treatment failure in leishmaniasis: A 21st century challenge. *PLoS Negl. Trop. Dis.* **11** (12), e0006052. <https://doi.org/10.1371/journal.pntd.0006052> (2017).
24. Pountain, A. W. et al. Genomic instability at the locus of sterol C24-methyltransferase promotes amphotericin B resistance in leishmania parasites. *PLoS Negl. Trop. Dis.* **13** (2), e0007052 (2019).
25. Ning, Y. et al. Lathosterol oxidase (sterol C-5 desaturase) deletion confers resistance to amphotericin B and sensitivity to acidic stress in leishmania major. *mSphere* **5** (4), e00380–e00320 (2020).
26. Alpizar-Sosa, E. A. et al. Amphotericin B resistance in leishmania Mexicana: alterations to sterol metabolism and oxidative stress response. *PLoS Negl. Trop. Dis.* **16** (9), e0010779. <https://doi.org/10.1371/journal.pntd.0010779> (2022).
27. Mwenechanya, R. et al. Sterol 14 α -demethylase mutation leads to amphotericin B resistance in leishmania Mexicana. *PLoS Negl. Trop. Dis.* **11** (6), e0005649 (2017).
28. Kaur, G. & Rajput, B. Comparative analysis of the omics technologies used to study antimonial, amphotericin B, and pentamidine resistance in leishmania. *J. Parasitol. Res.* **2014**, 1–11 (2014).
29. Brotherton, M. C. et al. Quantitative proteomic analysis of amphotericin B resistance in leishmania infantum. *Int. J. Parasitol. Drugs Drug Resist.* **4** (2), 126–132 (2014).
30. Singh, J. et al. L-asparaginase of leishmania donovani: metabolic target and its role in amphotericin B resistance. *Int. J. Parasitol. Drugs Drug Resist.* **7** (3), 337–349 (2017).
31. Singh, K. et al. Deciphering the interplay between cysteine synthase and thiol cascade proteins in modulating amphotericin B resistance and survival of leishmania donovani under oxidative stress. *Redox Biol.* **12**, 350–366 (2017).
32. Kumar, A. et al. Ascorbate peroxidase, a key molecule regulating amphotericin B resistance in clinical isolates of leishmania donovani. *Antimicrob. Agents Chemother.* **58** (10), 6172–6184 (2014).
33. Suman, S. S. et al. Up-regulation of cytosolic tryparedoxin in Amp B resistant isolates of leishmania donovani and its interaction with cytosolic tryparedoxin peroxidase. *Biochimie* **121**, 312–325 (2016).
34. Fernandez-Prada, C. et al. Different mutations in a P-type ATPase transporter in leishmania parasites are associated with cross-resistance to two leading drugs by distinct mechanisms. *PLoS Negl. Trop. Dis.* **10** (12), e0005171 (2016).
35. Perez-Franco, J. E. et al. Clinical and parasitological features of patients with American cutaneous leishmaniasis that did not respond to treatment with Meglumine antimoniate. *PLoS Negl. Trop. Dis.* **10** (5), e0004739. <https://doi.org/10.1371/journal.pntd.0004739> (2016).
36. van den Bogaart, E., Schoone, G. J., Adams, E. R. & Schallig, H. D. Duplex quantitative reverse-transcriptase PCR for simultaneous assessment of drug activity against leishmania intracellular amastigotes and their host cells. *Int. J. Parasitol. Drugs Drug Resist.* **4** (1), 14–19. <https://doi.org/10.1016/j.ijpddr.2013.11.001> (2013).
37. Wickham, H. *ggplot2: Elegant Graphics for Data Analysis* (Springer, 2016). <https://ggplot2.tidyverse.org>
38. Kassambara, A., Mundt, F. & factoextra Extract and visualize the results of multivariate data analyses. R package version 1.0.7 (2020). <https://CRAN.R-project.org/package=factoextra>
39. R Core Team. *R: A Language and Environment for Statistical Computing*. (R Foundation for Statistical Computing, 2023). <https://www.R-project.org/>
40. Tello, D. et al. NGSEP3: accurate variant calling across species and sequencing protocols. *Bioinformatics* **35** (22), 4716–4723 (2019).
41. Broad Institute. *Picard Toolkit*. (2019). <https://broadinstitute.github.io/picard/>
42. Letunic, I. & Bork, P. Interactive tree of life (iTOL) v5: An online tool for phylogenetic tree display and annotation. *Nucleic Acids Res.* **49**, W293–W296 <https://doi.org/10.1093/nar/gkab301> (2021).
43. Li, H. et al. 1000 Genome project data processing subgroup. The sequence alignment/map format and samtools. *Bioinformatics* **25** (16), 2078–2079. <https://doi.org/10.1093/bioinformatics/btp352> (2009).
44. Gutierrez Guarino, S. A., Tikhonova, E. B., Karamyshev, A. L., Muskus, C. E. & Karamysheva, Z. N. Translational reprogramming as a driver of antimony-drug resistance in leishmania. *Nat. Commun.* **14** (1), 2605. <https://doi.org/10.1038/s41467-023-38221-1> (2023).
45. Rastrojo, A. et al. Genomic and transcriptomic alterations in leishmania donovani lines experimentally resistant to antileishmanial drugs. *Int. J. Parasitol. Drugs Drug Resist.* **8** (2), 246–264. <https://doi.org/10.1016/j.ijpddr.2018.04.002> (2018).
46. Tripp, C. A., Myler, P. J. & Stuart, K. A DNA sequence (LD1) which occurs in several genomic organizations in leishmania. *Mol. Biochem. Parasitol.* **47** (2), 151–156. [https://doi.org/10.1016/0166-6851\(91\)90174-5](https://doi.org/10.1016/0166-6851(91)90174-5) (1991).
47. Collett, C. F. et al. Chemogenomic profiling of antileishmanial efficacy and resistance in the related kinetoplastid parasite trypanosoma brucei. *Antimicrob. Agents Chemother.* **63** (8), e00795–e00719. <https://doi.org/10.1128/AAC.00795-19> (2019).
48. Gazanion, É., Fernández-Prada, C., Papadopoulou, B., Leprohon, P. & Ouellette, M. Cos-Seq for high-throughput identification of drug target and resistance mechanisms in the protozoan parasite leishmania. *Proc. Natl. Acad. Sci.* **113** (21), E3012–E3021. <https://doi.org/10.1073/pnas.1520693113> (2016).
49. Ruy, P. C. et al. Comparative transcriptomics in leishmania Braziliensis: disclosing differential gene expression of coding and putative noncoding RNAs across developmental stages. *RNA Biol.* **16** (5), 639–660. <https://doi.org/10.1080/15476286.2019> (2019).
50. Vanerschot, M. et al. Linking in vitro and in vivo survival of clinical leishmania donovani strains. *PLoS One.* **5** (8), e12211. <https://doi.org/10.1371/journal.pone.0012211> (2010).
51. Pereira, L. O. R. et al. Insights from leishmania (Viannia) Guyanensis in vitro behavior and intercellular communication. *Parasit. Vectors.* **14** (1), 556. <https://doi.org/10.1186/s13071-021-05057-x> (2021).
52. Mano, C. et al. Amphotericin B resistance correlates with increased fitness in vitro and in vivo in leishmania (Mundinia) Martinicensis. *Front. Microbiol.* **14**, 1156061. <https://doi.org/10.3389/fmicb.2023.1156061> (2023).
53. Sampaio, M. C. et al. A 245 kb mini-chromosome impacts on leishmania Braziliensis infection and survival. *Biochem. Biophys. Res. Commun.* **382** (1), 74–78. <https://doi.org/10.1016/j.bbrc.2009.02.128> (2009).
54. Wu, Á. C. A. et al. Genetic differences between two leishmania major-like strains revealed by suppression subtractive hybridization. *Mol. Biochem. Parasitol.* **203** (1–2), 34–38. <https://doi.org/10.1016/j.molbiopara.2015.10.005> (2015).
55. Maharjan, M., Singh, S., Chatterjee, M. & Madhubala, R. Role of Aquaglyceroporin (AQP1) gene and drug uptake in antimony-resistant clinical isolates of leishmania donovani. *Am. J. Trop. Med. Hyg.* **79** (1), 69–75 (2008).
56. Maia, C. et al. In vitro drug susceptibility of leishmania infantum isolated from humans and dogs. *Exp. Parasitol.* **135** (1), 36–41. <https://doi.org/10.1016/j.exppara.2013.05.015> (2013).

57. Carnielli, J. B. T. et al. A leishmania infantum genetic marker associated with miltefosine treatment failure for visceral leishmaniasis. *EBioMedicine* **36**, 83–91. <https://doi.org/10.1016/j.ebiom.2018.09.029> (2018).
58. Carnielli, J. B. T. et al. 3'Nucleotidase/nuclease is required for Leishmania infantum clinical isolate susceptibility to miltefosine. *EBioMedicine* **86**, 104378. <https://doi.org/10.1016/j.ebiom.2022.104378> (2022).
59. Moreira, W., Leblanc, E. & Ouellette, M. The role of reduced pterins in resistance to reactive oxygen and nitrogen intermediates in the protozoan parasite leishmania. *Free Radic Biol. Med.* **46** (3), 367–375. <https://doi.org/10.1016/j.freeradbiomed.2008.10.034> (2009).
60. Reis-Cunha, J. L., Valdivia, H. O. & Bartholomeu, D. C. Gene and chromosomal copy number variations as an adaptive mechanism towards a parasitic lifestyle in trypanosomatids. *Curr. Genomics* **19** (2), 87–97. <https://doi.org/10.2174/1389202918666170911161311> (2018).
61. Ilgoutz, S. C., Zawadzki, J. L., Ralton, J. E. & McConville, M. J. Evidence that free GPI glycolipids are essential for growth of leishmania Mexicana. *EMBO J.* **18** (10), 2746–2755. <https://doi.org/10.1093/emboj/18.10.2746> (1999).
62. Juchimiuk, M. et al. Defect in dolichol-dependent glycosylation increase the sensitivity of *Saccharomyces cerevisiae* towards anti-fungal drugs. *Yeast* **27** (8), 637–645. <https://doi.org/10.1002/yea.1803> (2010).
63. Ribeiro, C. V., Rocha, B. F. B., Moreira, D. S., Peruhype-Magalhães, V. & Murta, S. M. F. Mannosyltransferase (GPI-14) overexpression protects promastigote and amastigote forms of leishmania *Braziliensis* against trivalent antimony. *Parasit. Vectors* **12** (1), 60. <https://doi.org/10.1186/s13071-019-3305-2> (2019).
64. Roberts, A. et al. The leishmania donovani ortholog of the glycosylphosphatidylinositol anchor biosynthesis cofactor PBN1 is essential for host infection. *mBio* **13** (3), e0043322. <https://doi.org/10.1128/mbio.00433-22> (2022).

Acknowledgements

The work presented in this manuscript was supported by MinCiencias [Patrimonio autónomo del Fondo Nacional de Financiamiento para la ciencia, la tecnología y la innovación Francisco José de Caldas. Contract 80740-441-2020] and Universidad Nacional de Colombia internal grant-HERMES number 57759. We acknowledge the High-Performance Computing Service at Universidad de los Andes at Bogotá, Colombia, for providing HPC resources that have contributed to the research results reported in this paper. We also thank Mr. Alejandro Contreras from the Parasitology Lab., Facultad de Medicina, Universidad Nacional, for the technical support.

Author contributions

JD, MCE, and LNGG conceived the study and coordinated the project. LNGG, AMRG, CMVL, SA, LABV, JMMG, AMC, GADO, and CAB collected the data and performed lab work. LNGG, JD, MCE, DAU, CMVL, and AMRG performed bioinformatic analysis and interpretation of the results. LNGG, MCE, and JD drafted the manuscript. All authors reviewed and approved the latest version of the manuscript.

Declarations

Competing interests

The authors declare no competing interests.

Additional information

Supplementary Information The online version contains supplementary material available at <https://doi.org/10.1038/s41598-025-96849-z>.

Correspondence and requests for materials should be addressed to M.C.E.

Reprints and permissions information is available at www.nature.com/reprints.

Publisher's note Springer Nature remains neutral with regard to jurisdictional claims in published maps and institutional affiliations.

Open Access This article is licensed under a Creative Commons Attribution-NonCommercial-NoDerivatives 4.0 International License, which permits any non-commercial use, sharing, distribution and reproduction in any medium or format, as long as you give appropriate credit to the original author(s) and the source, provide a link to the Creative Commons licence, and indicate if you modified the licensed material. You do not have permission under this licence to share adapted material derived from this article or parts of it. The images or other third party material in this article are included in the article's Creative Commons licence, unless indicated otherwise in a credit line to the material. If material is not included in the article's Creative Commons licence and your intended use is not permitted by statutory regulation or exceeds the permitted use, you will need to obtain permission directly from the copyright holder. To view a copy of this licence, visit <http://creativecommons.org/licenses/by-nc-nd/4.0/>.

© The Author(s) 2025